DOI: 10.1002/chem.200902968

# Identifying the Bond Responsible for the Fluorescence Modulation in an Amyloid Fibril Sensor

**Anvita Srivastava,[a, c] Prabhat K. Singh,[a] Manoj Kumbhakar,[a] Tulsi Mukherjee,[a] Subrata Chattopadyay,[b] Haridas Pal,[a] and Sukhendu Nath*[a]**

**Abstract:** An ultrafast intramolecular bond twisting process is known to be the responsible mechanism for the sensing activity of the extensively used amyloid fibril sensor thioflavin T (ThT). However, it is not yet known which one of the two possible single bonds in ThT is actually involved in the twisting process. To resolve this fundamental issue, two derivatives of ThT have been designed and synthesized and subsequently their photophysical properties have been studied in different solvents. It is understood from the present study that the rotation around the central C–C single bond, and not that around the C–N single bond, is primarily responsible for the sensor activity of ThT. Detailed viscosity-dependent fluorescence studies revealed that the ThT derivative with restricted C–N bond rotation acts as a better sensor than the derivative with free C–N bond rotation. The better sensory activity is directly correlated with a shorter excited-state lifetime. Results obtained from the photophysical studies of the ThT derivatives have also been supported by the results obtained from quantum chemical calculations.

**Keywords:** sensors · bond twisting · fluorescence · thioflavin T · time-resolved spectroscopy

## Introduction

The existence of protein molecules in their native structural form is very essential for their normal biological activities. A significant departure from their native structural forms leads to several diseases. For example, misfolding of protein molecules can lead to their association and ultimately formation of insoluble protein aggregates. The presence of such aggregated protein molecules in brain, known as amyloid fibrils, results in the several neurodegenerative disorders, like Alzheimer's and Parkinson's diseases.[1–5] To detect and control such protein-related diseases, it is very essential to monitor the progress of protein aggregation, which ultimately leads to the fibril formation. Among several techniques used to monitor and detect the amyloid fibril formation, the use of an extrinsic fluorescence probe is found to be very extensive.[6–10]

Thioflavin T (ThT), a benzothiazole-based cationic dye (see Scheme 1) is one of the frequently used extrinsic fluorescent probes to study the formation and detection of amyloid fibrils.[11–14] ThT is known to specifically bind to the proteins when the latter is in the form of amyloid fibril, but not in their native structural form.[15,16] The emission yield of ThT in water is extremely low[17,18] but shows a large enhancement on binding with amyloid fibrils.[2,12,15,19–22] The underlying mechanism for the extremely large fluorescence enhancement for ThT associated with amyloid fibril is still

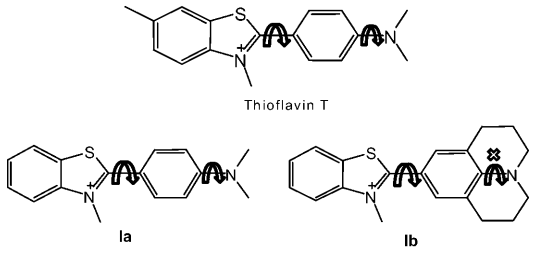


Scheme 1. Molecular structure of thioflavin T and its derivatives used in the present study.

[a] A. Srivastava, P. K. Singh, Dr. M. Kumbhakar, Dr. T. Mukherjee, Dr. H. Pal, Dr. S. Nath
Radiation & Photochemistry Division
Bhabha Atomic Research Centre, Trombay
Mumbai-400 085 (India)
Fax: (+91) 22-5505151
E-mail: snath@barc.gov.in

[b] Dr. S. Chattopadyay
Bio-Organic Division
Bhabha Atomic Research Centre, Trombay
Mumbai-400 085 (India)

[c] A. Srivastava
Department of Chemistry, University of Allahabad
Allahabad, Utter Pradesh-211 002 (India)

   

unknown. However, several hypotheses have been proposed in the literature to explain this phenomenon. Formation of ThT micelles in the environment of the amyloid fibril have been proposed by Khurana et al.[23] Groenning et al.[24] have proposed that the formation of ThT excimers in the excited state is mainly responsible for the observed fluorescence enhancement, though the formation of excimers by a charged species is always a topic of debate. Very recently, by using optical microscopic measurements, Kitts and Vanden Bout[25] have shown that the observed enhancement in the emission of the ThT in amyloid fibril is due to the association of the monomeric form of the dye to the protein rather than the formation of their micelles or excimers.

Detailed studies in several confined environments, like in amyloid fibril,[2,12,15,19–22] polymer,[26] glass matrix,[27] nanoconfined water pool,[18] etc., clearly indicate that the high local viscosity of the microenvironment around the dye is directly related to the observed fluorescence enhancement of the ThT dye in these systems. However, understanding the basic molecular process that is associated with the observed fluorescence enhancement of ThT in the above microenvironments remains elusive. Considering the molecular structure of ThT, it is hypothesized that in bulk water, due to the low viscosity of the medium, some intramolecular bond twisting process takes place in the excited state of the ThT molecules. This bond twisting process effectively introduces a very fast nonradiative decay channel for the excited ThT molecule, which leads to its extremely low emission yield. In contrast, in a highly viscous medium, like in amyloid fibril, the bond twisting process in the dye is substantially retarded, reducing the nonradiative decay channel in its excited state. This results in a remarkable increase in the emission yield of ThT in a highly viscous medium. It is also proposed that the bond twisting process is associated with the large intramolecular charge transfer from the aniline moiety of ThT to the benzothiazole moiety.[28,29] Such a charge transfer, associated with the bond twisting in the dye, effectively results in the formation of a twisted intramolecular charge transfer (TICT) state in the excited ThT molecules.

From the molecular structure of ThT (see Scheme 1), it is clearly evident that there are two possible bond twistings, one occurring around the C–N single bond (i.e., twisting of the amino ($NR_2$) group) and/or the other occurring around the central C–C single bond (i.e., twisting of the anilino ($PhNR_2$) group). Twisting around any one of these bonds can introduce the nonradiative decay channel in the excited state of ThT, causing a very low emission yield. There are several reports in the literature on organic dyes with an N-alkylated anilino group where it is shown that the twisting of either the N-alkylated amino group or of the anilino group can cause the enhanced nonradiative decay of the excited dye that results in a large reduction of their emission yields. For example, in several triphenyl dyes with amine substitution, it is reported that the twisting of the anilino group in their excited state is responsible for their low emission yield.[30,31] For *para*-(*N*,*N*-dialkylamino)benzylidenemalononitriles, however, based on experimental evidence as well as from theoretical calculations, it was shown that the twisting of the amino group as well as of the anilino group contribute significantly towards the nonradiative decay channel of this molecule in its excited states.[32] Very recently, Saha et al.[33] have shown that in dimethyl-aminostyrylbenzothiazole, having a close structural relation with ThT, only the twisting of the amino group is responsible for the fast nonradiative decay in its excited state.

Based on these literature precedents, it is expected that for ThT twisting of either of these two bonds (see Scheme 1) can be responsible for the ultrafast nonradiative decay channel in its excited state. In order to use ThT or some of its derivatives as an efficient sensor for different microenvironments, including that of amyloid fibril, it is very essential to identify the bond, which is responsible for its ultrafast nonradiative decay channel. This information might also help to develop much better sensor based on the ThT structure. In order to disentangle this issue, we designed and synthesized two ThT derivatives, **Ia** and **Ib** (Scheme 1), with the premise that the lack of a methyl group in the benzothiazole, as is present in ThT, would not change the fluorescence properties, compared to ThT. For the two dye molecules, twisting around both bonds is possible in **Ia**, but the presence of a julolidine group in **Ib** would prohibit twisting of the Ph–$NR_2$ bond and allows twisting around the central C–C bond (benzothiazole–aniline) only. Subsequently, we carried out detailed steady-state and time-resolved photophysical studies of **Ia** and **Ib** in different solvents to identify the bond that is responsible for the sensory activity of the ThT class of molecules. The experimental results are also substantiated by quantum chemical calculations.

## Results and Discussion

**Steady-state absorption and fluorescence studies**: The ground-state absorption and the steady-state fluorescence spectra of the ThT derivatives **Ia** and **Ib** in aqueous solution are shown in Figure 1. As indicated in the Figure, both absorption and emission spectra of **Ib** are significantly red

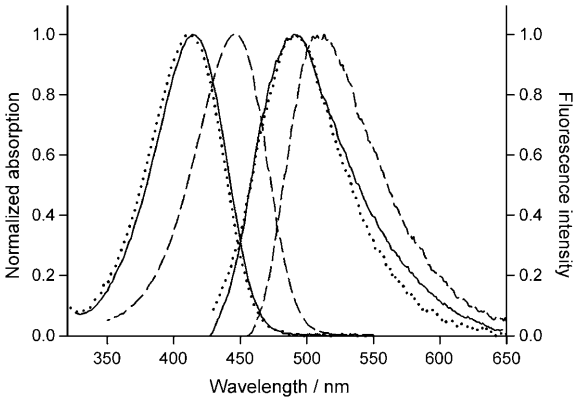


Figure 1. Ground-state absorption and steady-state fluorescence spectra of **Ia** (——) and **Ib** (-----) in aqueous solution. Absorption and emission spectra of ThT in water (•••••) are also shown for comparison.

  

shifted with respect to those of **Ia**. This red shift is possibly due to the fact that the difference in the ground-state and the excited-state dipole moment is higher for the former dye as compared to that in the latter. The more polar nature of the dye **Ib** as compared to that of dye **Ia** is a result of the presence of the julolidine group in the former. The red shift of the absorption maxima in dye **Ib** compared to dye **Ia** is also supported by the quantum chemical calculations (see latter). Similar red shifts in the absorption and emission spectra due to the introduction of the julolidine group have also been observed in coumarin derivatives.[34] As anticipated, the absorption and the emission spectral characteristics of **Ia** in water (and also in other solvents) were quite similar to that of ThT (see Figure 1). This clearly supports our proposed hypothesis on the inconsequential role of the methyl substitution in the benzene ring of the benzothiazole unit in the photophysical properties of the ThT molecules.

Fluorescence quantum yield values have been measured for both the ThT derivatives in different solvents and are listed in Table 1. The quantum yield values of ThT in different solvents are also presented in Table 1 for comparison. It is evident from Table 1 that the quantum yield of ThT and **Ia** are quite comparable in all solvents studied. This result indicates that ThT and its derivative **Ia** have similar photophysical behavior, which is consistent with our inference from the absorption and emission spectral studies. Thus, henceforth the dye **Ia** will be considered as a representative of ThT and its photophysical properties will be compared with those of **Ib**.

Table 1. Emission quantum yields ($\phi_f$) of ThT, **Ia**, and **Ib** in different solvents.

| Solvent | Quantum yield ($\phi_f$) $\times 10^4$ | | |
|---|---|---|---|
| | ThT | **Ia** | **Ib** |
| water | $1.0 \pm 0.2$ | $1.0 \pm 0.2$ | $0.84 \pm 0.2$ |
| acetonitrile | $1.42 \pm 0.15$ | $1.45 \pm 0.2$ | $0.84 \pm 0.15$ |
| ethylene glycol | $17.5 \pm 0.5$ | $16.1 \pm 0.4$ | $10.1 \pm 0.5$ |

It is clearly indicated from Table 1 that the introduction of the julolidine group in **Ib** to prevent the twisting around the C–N bond does not cause any appreciable changes in the emission yield of the dye as compared to that of **Ia** and ThT. Further, it can be seen that the emission yield of **Ib** is always relatively less as compared to that of **Ia** and ThT in all the solvents studied. As reported in the literature, the restriction of the bond rotation in ThT in viscous environment, like in amyloid fibril, is the reason for the observed large enhancement ($\approx$1000 times) in the fluorescence yield.[2,12,15,19–22,35] If the restriction in the rotation around C–N bond is responsible for the sensing activity of ThT, one would expect a large increase in the emission quantum yield for the dye **Ib** in comparison to that of **Ia** and ThT. Lack of any such enhancement in the fluorescence yield of **Ib** clearly suggests that the twisting around the C–N bond is not responsible for the sensory activity of the ThT molecules. This, in turn, revealed that the twisting around the central C–C single bond (i.e., the twisting of the anilino group) is mainly responsible for the fluorescence sensing activity of the ThT dye.

As the sensing activity of ThT is related to the bond twisting process, the emission quantum yield of the two ThT derivatives **Ia** and **Ib**, is expected to be highly dependent on the viscosity of the medium. To investigate this aspect, we measured the fluorescence quantum yields of **Ia** and **Ib** in solvent mixtures of acetonitrile–ethylene glycol in different proportions so that the viscosity of the medium can be changed over a wide range.[36] The reason for selecting acetonitrile–ethylene glycol as solvent mixture is to maintain the polarity of the medium while varying the composition of the co-solvents. As charge separation takes place in the excited state of these molecules, the polarity of the medium can affect its fluorescence quantum yield.[28] The dielectric constant of acetonitrile and ethylene glycol are in the similar range ($\varepsilon \approx 37$).[37] Further, to see the fluorescence enhancement at the higher viscosity region, the fluorescence yields of the two dyes were also measured in glycerol at different temperatures.[38,39] It is to be mentioned, that for ThT it is reported that its fluorescence quantum yield in solvents with high dielectric constants, like acetonitrile, methanol, and water, is almost independent of the solvent polarity.[17] In the present study, we also find similar fluorescence quantum yields for **Ia** and **Ib** in water and acetonitrile (see Table 1). Thus, it is expected that within this high solvent polarity region the TICT-mediated nonradiative de-excitation of the excited **Ia** and **Ib** molecules is not affected significantly by the small changes in the solvent polarity. Thus, a marginally higher dielectric constant of glycerol ($\varepsilon \approx 42.5$) as compared to that of acetonitrile and ethylene glycol should not affect the fluorescence quantum yield of these dyes, rather the viscosity of the solvent will play a significant role in modulating their photophysical behavior. The variation of the fluorescence quantum yields (relative to that in acetonitrile) of **Ia** and **Ib** with the viscosity of the medium is shown in Figure 2. It is clearly indicated from the inset of Figure 2

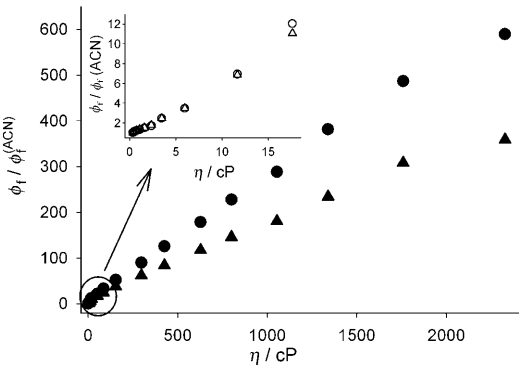


Figure 2. Variation of fluorescence quantum yield (relative to that in acetonitrile) of **Ia** (△) and **Ib** (○) with the viscosity of the medium. The inset shows the variation in the emission yield for the low solvent viscosity region. Open symbol corresponds to acetonitrile–ethylene glycol mixtures and filled symbol corresponds to glycerol solutions with different viscosity (varied by changing the temperature).

  

that in the low-viscosity region (<20 cP) the fluorescence enhancement due to the increase in the viscosity is very similar for both of the dyes. However, a substantial difference in the fluorescence enhancement was observed in the region of higher solvent viscosity, where the rate of change in the fluorescence quantum yield with the solvent viscosity is relatively higher for **Ib** compared to that for **Ia**. This result clearly demonstrates that **Ib** is a relatively better viscosity sensor than **Ia**.

**Time-resolved fluorescence studies**: The fundamental issue that determines the sensing activity of a fluorescence dye is the competition between the radiative and nonradiative (due to the bond twisting) decay processes in the excited state of the dye molecules. The fluorescence quantum yield, $\phi_f$, of a dye is defined by the following Equation (1),

$$\phi_f = \frac{k_f}{k_f + k_{nr} + k_{nr}^{tor}} = \tau_f k_f \quad (1)$$

where $k_f$ is the radiative rate constant, $k_{nr}$ is the nonradiative rate constant for processes other than bond twisting process, $k_{nr}^{tor}$ is the nonradiative rate constant due to the bond twisting process, and $\tau_f (= 1/k_f + k_{nr} + k_{nr}^{tor})$ is the excited-state lifetime of the dye. In a less viscous solvent, for example water, the intramolecular bond twisting process is very efficient for ThT and thus, leads to a higher value for $k_{nr}^{tor}$, resulting in a very low $\tau_f$ value. Because of the very high $k_{nr}^{tor}$ value, the quantum yield $\phi_f$ is also very low in low viscous solvent. However, in highly viscous media, the bond twisting process is retarded significantly, resulting in a lower $k_{nr}^{tor}$ value and subsequently a higher $\phi_f$ value for the dye. Thus, to understand the difference in the sensing activity of **Ia** and **Ib**, time-resolved fluorescence measurements were carried out in different solvents by using the fluorescence upconversion technique. Both dyes show multi-exponential fluorescence decay behavior at their emission maxima in all the solvents studied. Multi-exponential decay kinetics for the barrierless bond twisting process is well known in the literature.[40,41] The representative fluorescence decays of **Ia** and **Ib** in ethylene glycol are shown in Figure 3, whereas their estimated average fluorescence lifetimes in different solvents are presented in Table 2. It is evident from Figure 3 and also from Table 2 that the average lifetime of **Ia** is always longer as compared to that of **Ib** in all the solvents studied. The observed ultrafast decay is known to be due to the torsional motion in the ThT dyes.[18] Thus, the present results clearly indicate that the torsional motion is relatively faster in **Ib** compared to **Ia**. Accordingly, the $k_{nr}^{tor}$ value is always higher for **Ib** than that for **Ia** irrespective of the solvent used. Because of the larger value of $k_{nr}^{tor}$ and hence, lower value of $\tau_f$, the increase in fluorescence yield due to an increase in the solvent viscosity is expected to be relatively higher for **Ib** than for **Ia**. Hence, the observed larger enhancement in fluorescence quantum yield of the dye **Ib** with an increase in the solvent viscosity as compared to that of dye **Ia** is attributed to the faster bond twisting process in the former dye.

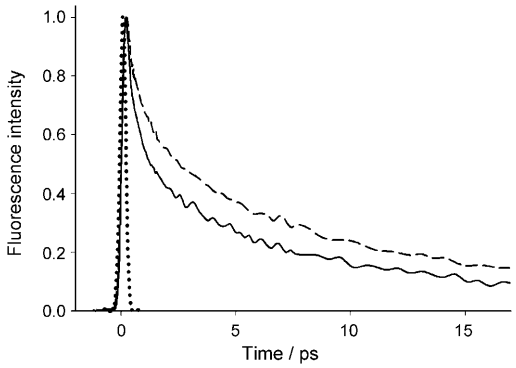


Figure 3. Transient fluorescence decays of **Ia** (-----, $\lambda_{ex}$=410 nm, $\lambda_{em}$= 490 nm) and **Ib** (——, $\lambda_{ex}$=420 nm, $\lambda_{em}$=510 nm) in ethylene glycol solution. The instrument response function (IRF) is shown as the dotted curve.

Table 2. Average excited state lifetime of **Ia** and **Ib** in different solvents.

| Solvent | Average fluorescence lifetime [ps] | |
|---|---|---|
| | **Ia** | **Ib** |
| water | 0.59 | 0.48 |
| acetonitrile | 0.41 | 0.30 |
| ethylene glycol | 12.4 | 11.8 |

**Quantum-chemical calculations**: To understand the reason behind the faster bond twisting dynamics in **Ib** as compared to **Ia**, detailed quantum-chemical calculations were carried out. The structure of both molecules were optimized by applying DFT using the B3LYP functional and are shown in Figure 4.

From the optimized structures of both dyes it is evident that these molecules are non-planner in nature. The plane containing the benzothiazole moiety undergoes a twist of

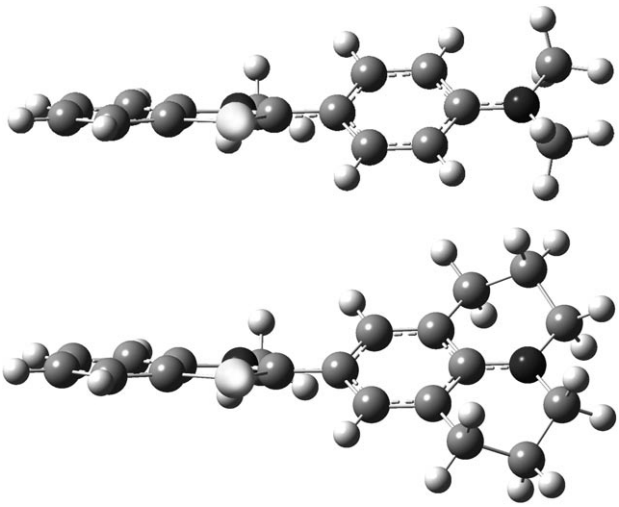

Figure 4. Optimized chemical structures of **Ia** (top) and **Ib** (bottom).

  

about 40° for **Ia** and about 36° for **Ib** with respect to the plane of anilino moiety. Vertical transition energies were also calculated for the optimized geometry for these two molecules and were found to be approximately 3.055 eV (406 nm) and approximately 2.893 eV (428 nm) for **Ia** and **Ib**, respectively. These values correspond reasonably well with the experimentally observed absorption maxima (412 nm and 440 nm for **Ia** and **Ib**, respectively).

To understand how the dihedral angle ($\theta_B$) between the benzothiazole and the anilino moieties affect the potential energy surface of the two molecules, both ground-state and excited-state potential energies were calculated for different values of $\theta_B$ and are shown as in Figure 5. It is evident from Figure 5 that for both dyes the locally excited state (with

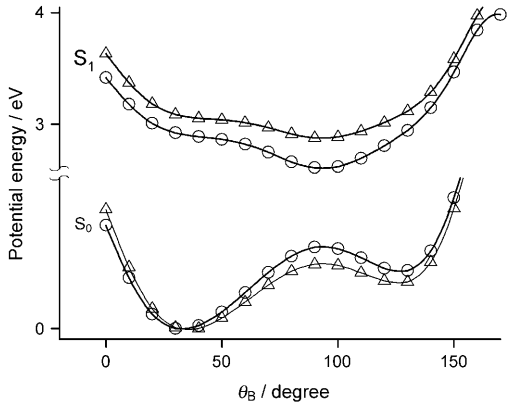


Figure 5. Variation in the potential energy of **Ia** (△) and **Ib** (○) with the dihedral angle $\theta_B$ in their ground state ($S_0$) and the first excited state ($S_1$). The calculated energy is relative to the minimum of the ground-state energy.

$\theta_B = 40°$ for **Ia** and 36° for **Ib**), produced due to photoexcitation, does not correspond to the energetically minimum in the potential energy surface. Thus, both molecules undergo bond twisting around the C–C single bond between the benzothiazole and the anilino moiety to attain a $\theta_B$ value of $\approx 90°$ in their excited state to attain the minimum in the potential energy surface. This feature is qualitatively very similar to that obtained for the ThT molecules in the gas phase.[28]

Although the qualitative nature of the potential energy surfaces of **Ia** and **Ib** are very similar, there are distinct quantitative differences between them, which can explain the observed differences in the excited-state dynamics of these two molecules. It is to be noted from Figure 5 that the energy stabilization due to a bond twisting process in the excited state is relatively higher for **Ib** than for **Ia**, suggesting that the twisting process occurs faster in the former. Further, the excited-state potential energy surface in the region of $\theta_B = 40$–90° is relatively steeper for **Ib** than that for **Ia**. This feature also suggests a faster bond twisting process in **Ib** than in **Ia**. In addition, it is also evident from the Figure 5 that the energy gap between the $S_1$ and $S_0$ states at the twisted configuration (i.e., $\theta_B = 90°$) is relatively small for **Ib** as compared to that in **Ia**. This lower energy gap between the $S_1$ and the $S_0$ state also causes the nonradiative process to be more efficient in **Ib** than in **Ia**. Thus, because of all above factors, the fluorescence lifetime of **Ib** is expected to be shorter than the one of **Ia**, which is also observed experimentally. Therefore, the results of the quantum chemical calculation are in good agreement with the observed experimental results and support the role of the bond twisting process around the central C–C single bond to cause the extremely low fluorescence quantum yield of the ThT dyes and its derivatives.

## Conclusion

In conclusion, from detail photophysical studies of two newly synthesized ThT derivatives it is inferred that the C–N bond twisting is not responsible for the sensing activity of ThT and its derivatives. The twisting around the central C–C single bond between the benzothiazole and the anilino moieties appears to be mainly responsible for the observed fluorescence sensing activity of these dyes. Detailed viscosity-dependent studies show that dye **Ib** with a julolidine substituent acts as a better sensor than dye **Ia**. The better sensing activity of **Ib** is found to be due to a faster nonradiative decay rate of the excited state. The faster nonradiative process in **Ib** is also predicted by the quantum chemical calculations.

## Experimental Section

**Absorption and fluorescence spectral studies**: Ground-state absorption and steady-state fluorescence measurements were carried out with a Shimadzu (Japan, model UV-160A) spectrophotometer and Hitachi (Japan, model 4010F) spectrofluorimeter, respectively. The fluorescence spectra were corrected for the wavelength-dependent instrument responses by measuring the spectrum of quinine sulfate and comparing it with the reported standard spectrum.[42] The fluorescence quantum yield ($\phi_f$) of **Ia** and **Ib** were measured by comparison methods,[43] using coumarin-481 in acetonitrile ($\phi_f = 0.08$[44]) as standard.

**Time-resolved fluorescence studies**: Time-resolved emission measurements were carried out with a femtosecond Ti–sapphire laser-based fluorescence upconversion instrument that has been described earlier.[45] Briefly, a second harmonic laser pulse of Ti–sapphire laser ($\approx$50 fs at full width at half maximum (FWHM)) was used for the excitation of the sample. The fluorescence light from the sample was collected and focused onto a 0.5 mm thick β-barium borate (BBO) crystal by using a pair of parabolic mirrors. The fundamental laser pulse (gate pulse), after passing through an optical delay rail, was mixed with the fluorescence light into the BBO crystal to generate the sum frequency light, which was detected by using a photon counter after passing through a double monochromator. To obtain the fluorescence decay of the sample, the sum frequency light was detected as a function of the delay time between the gate and the excitation pulse. The instrument response function (IRF) of the present setup were measured through cross correlation between the gate pulse and second harmonic excitation pulse and found to be 230 fs. Decay traces were monitored at the emission maximum of the respective dye, that is, 490 nm for **Ia** and 510 nm for **Ib**. It is to be mentioned that the decay traces for both dyes are seen to be independent of the excitation wavelength.

  

**Quantum-chemical calculation**: The ground-state geometry optimization of **Ia** and **Ib** was performed by using the density functional theory (DFT). Becke's three parameter hybrid exchange function with the Lee–Yang–Parr gradient corrected correlated functional (B3LYP)[46,47] was used in conjunction with the 6-311+G(d,p) basis set as implemented in the Gaussian 03 software package.[48] The conductor-like polarizable continuum model (CPCM)[49] was used to incorporate the effect of the bulk solvent (water). TDDFT method by using B3LYP/6–311+ G(d,p) basis set was used to calculate the energy in the excited state of the two dyes at different dihedral angle. The energy of the first excited singlet state ($S_1$) was determined as the sum of the ground state ($S_0$) energy and the transition energy. The energy (expressed in eV) is relative to the minimum of the ground-state energy.

**Synthesis of Ia and Ib**: The syntheses of **Ia** and **Ib** are outlined in Scheme 2. All anhydrous reactions were carried out under an argon atmosphere by using freshly dried solvents. The organic extracts were dried over anhydrous $Na_2SO_4$. The $^1$H NMR (200 MHz) spectra were recorded with a Bruker AC-200 spectrometer.

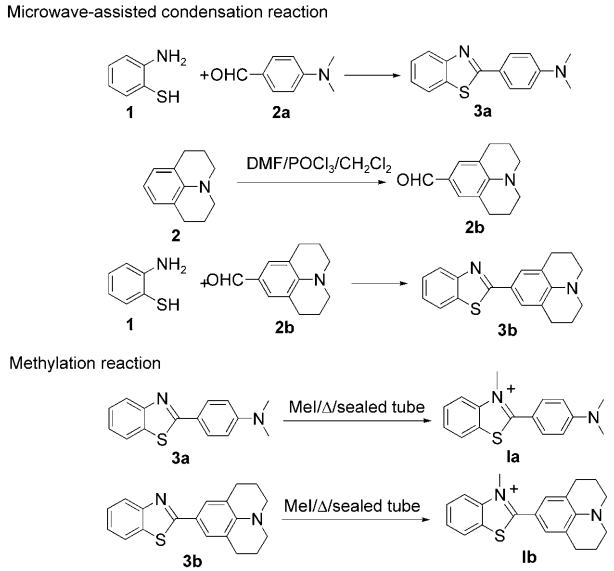


Scheme 2. Synthesis of **Ia** and **Ib**.

**Synthesis of 9-formyljulolidine (2b)**: To a magnetically stirred solution of julolidine (**2**) (0.5 g, 2.88 mmol) and DMF (0.27 mL, 3.46 mmol) in dry $CH_2Cl_2$ (5 mL) under argon was injected $POCl_3$ (0.29 mL, 3.17 mmol). After 1 h, when the substrate was fully consumed (as determined by TLC), the mixture was treated with aqueous solution of NaOH (2 M, 5 mL) and the mixture was extracted with $Et_2O$ (3×5 mL). The ether layer was washed with water (2×10 mL) and brine (1×5 mL) and dried. Removal of the solvent in vacuum followed by column chromatography (silica gel, 0–5% $Et_2O$/hexane) of the residue furnished pure **2b** (0.52 g, 90%). $^1$H NMR (200 MHz, $CDCl_3$): $\delta$=1.97–2.06 (m, 4H), 2.81 (t, $J$=6.2 Hz, 4H), 3.31 (t, $J$=5.8 Hz, 4H), 7.28 (s, 2H), 9.63 ppm (s, 1H).

**Synthesis of 2-(4′-diaminophenyl)benzothiazole (3a) and julolidinyl benzothiazole (3b)**: The aldehyde **2a** or **2b** (3 mmol) and 2-aminothiophenol (**1**) (6.0 mM) in $Et_2O$ (10 mL) and silica gel (3.0 g) were thoroughly mixed to make slurry, and concentrated under vacuum to obtain the respective solid preadsorbed materials, which were individually exposed to microwave irradiation (600 W) for 10 min. The completion of the reaction was checked by taking an aliquot of the sample, extracting it with $Et_2O$ and carrying out TLC analysis of the ether extract. The solid was extracted with $Et_2O$ (30 mL), the ether extract concentrated in vacuum, and the residue was purified by column chromatography (silica gel, 0–15% EtOAc/hexane) to obtain the respective 2-arylbenzothiazoles **3a** (0.685 g, 90%) and **3b** (0.629 g. 68.5%). **3a**: $^1$H NMR (200 MHz, $CDCl_3$): $\delta$=3.05 (s, 6H), 6.74 (d, $J$=9.0 Hz, 2H), 7.25–7.34 (m, 1H), 7.40–7.48 (m, 1H), 7.84 (d, $J$=7.8 Hz, 1H), 7.95–8.01 ppm (m, 3H); **3b**: $^1$H NMR (200 MHz, $CDCl_3$): $\delta$=1.92–2.04 (m, 4H), 2.81 (t, $J$=6.2 Hz, 4H), 3.26 (t, $J$=5.8 Hz, 4H), 7.26–7.32 (m, 1H), 7.39–7.46 (m, 1H), 7.59 (s, 2H), 8.03 (d, $J$=8.0 Hz, 1H), 7.79 ppm (d, $J$=8.0 Hz, 1H).

**Synthesis of the dyes Ia and Ib**: A mixture of **3a** or **3b** (each 0.2 g) and MeI (2 equiv) was heated at 120°C in a sealed tube for 4 h. The mixture was concentrated in vacuum, and the crude products were washed successively with acetone (3 mL) and $Et_2O$ (3 mL) and recrystallized from ethanol to give the desired products **Ia** (0.135 g, 63%) and **Ib** (0.125 g, 60%). **Ia**: $^1$H NMR (200 MHz, [D$_6$]DMSO): $\delta$=3.10 (s, 6H), 4.22 (s, 3H), 6.97 (d, $J$=8.4 Hz, 2H), 7.75–7.83 (m, 4H), 8.28–8.38 ppm (m, 2H); **Ib**: $^1$H NMR (200 MHz, [D$_6$]DMSO): $\delta$=1.86–1.91 (m, 4H), 2.72–2.78 (m, 4H), 3.54 (m, 4H), 4.18 (s, 3H), 7.38 (s, 2H), 7.64–7.83 (m, 2H), 8.09–8.12 (m, 1H), 8.26–8.30 ppm (m, 1H).

## Acknowledgements

The authors wish to thank Dr. S. K. Sarkar, Head, Radiation & Photochemistry Division, for his constant encouragement and support during this work and Prof. A. Dutta, Indian Institute of Technology, Bombay, for his help in the quantum chemical calculations. One of the authors (A.S.) is thankful to the Indian Science Academies (IASC, INSA & NASI) for the summer research fellowship.

[1] J. D. Harper, P. T. Lansbury, *Annu. Rev. Biochem.* **1997**, *66*, 385–407.
[2] F. Chiti, C. M. Dobson, *Annu. Rev. Biochem.* **2006**, *75*, 333–366.
[3] R. N. Rambaran, L. C. Serpell, *Prion* **2008**, *2*, 112–117.
[4] A. M. Damas, M. J. Saraiva, *J. Struct. Biol.* **2000**, *130*, 290–299.
[5] E. Zerovnik, *Eur. J. Biochem.* **2002**, *269*, 3362–3371.
[6] T. Ban, K. Yamaguchi, Y. Goto, *Acc. Chem. Res.* **2006**, *39*, 663–670.
[7] M. Lindgren, K. Sörgjerd, P. Hammarström, *Biophys. J.* **2005**, *88*, 4200–4212.
[8] K. D. Volkova, V. B. Kovalska, A. O. Balanda, R. J. Vermeij, V. Subramaniam, Y. L. Slominskii, S. M. Yarmoluk, *J. Biochem. Biophys. Methods* **2007**, *70*, 727–733.
[9] M. R. Nilsson, *Methods* **2004**, *34*, 151–160.
[10] A. Hawe, M. Sutter, W. Jiskoot, *Pharm. Res.* **2008**, *25*, 1487–1499.
[11] J. E. Gestwicki, G. R. Crabtree, I. A. Graef, *Science* **2004**, *306*, 865–869.
[12] C. Cabaleiro-Lago, F. Quinlan-Pluck, I. Lynch, S. Lindman, A. M. Minogue, E. Thulin, D. M. Walsh, K. A. Dawson, S. Linse, *J. Am. Chem. Soc.* **2008**, *130*, 15437–15443.
[13] S. Gilead, E. Gazit, *Angew. Chem.* **2004**, *116*, 4133–4136; *Angew. Chem. Int. Ed.* **2004**, *43*, 4041–4044.
[14] U. J. Shukla, H. Marino, P. S. Huang, S. L. Mayo, J. J. Love, *J. Am. Chem. Soc.* **2004**, *126*, 13914–13915.
[15] H. LeVine III, *Protein Sci.* **1993**, *2*, 404–410.
[16] V. Vetri, C. Canale, A. Relini, F. Librizzi, V. Militello, A. Gliozzi, M. Leone, *Biophys. Chem.* **2007**, *125*, 184–190.
[17] A. A. Maskevich, V. I. Stsiapura, V. A. Kuzmitsky, I. M. Kuznetsova, O. I. Povarova, V. N. Uversky, K. K. Turoverov, *J. Proteome Res.* **2007**, *6*, 1392–1401.
[18] P. K. Singh, M. Kumbhakar, H. Pal, S. Nath, *J. Phys. Chem. B* **2009**, *113*, 8532–8538.
[19] H. Yagi, T. Ban, K. Morigaki, H. Naiki, Y. Goto, *Biochemistry* **2007**, *46*, 15009–15017.
[20] R. L. Yona, S. Mazeres, P. Faller, E. Gras, *ChemMedChem* **2008**, *3*, 63–66.
[21] A. Abedini, F. Meng, D. P. Raleigh, *J. Am. Chem. Soc.* **2007**, *129*, 11300–11301.
[22] G. Soldi, F. Bemporad, F. Chiti, *J. Am. Chem. Soc.* **2008**, *130*, 4295–4302.

  

[23] R. Khurana, C. Coleman, C. Ionescu-Zanetti, S. A. Carter, V. Krishna, R. K. Grover, R. Roy, S. Singh, *J. Struct. Biol.* **2005**, *151*, 229–238.
[24] M. Groenning, L. Olsen, M. van de Weert, J. M. Flink, S. Frokjaer, F. S. Jørgensen, *J. Struct. Biol.* **2007**, *158*, 358–369.
[25] C. C. Kitts, D. A. Vanden Bout, *J. Phys. Chem. B* **2009**, *113*, 12090–12095.
[26] C. R. Raj, R. Ramaraj, *Photochem. Photobiol.* **2001**, *74*, 752–759.
[27] R. Schirra, *Chem. Phys. Lett.* **1985**, *119*, 463–466.
[28] V. I. Stsiapura, A. A. Maskevich, V. A. Kuzmitsky, K. K. Turoverov, I. M. Kuznetsova, *J. Phys. Chem. A* **2007**, *111*, 4829–4835.
[29] V. I. Stsiapura, A. A. Maskevich, V. A. Kuzmitsky, V. N. Uversky, I. M. Kuznetsova, K. K. Turoverov, *J. Phys. Chem. B* **2008**, *112*, 15893–15902.
[30] M. Jurczok, P. Plaza, M. M. Martin, W. Rettig, *J. Phys. Chem. A* **1999**, *103*, 3372–3377.
[31] M. Vogel, W. Rettig, *Ber. Bunsen-Ges.* **1985**, *89*, 962–968.
[32] R. O. Loutfy, *Macromolecules* **1981**, *14*, 270–275.
[33] S. K. Saha, P. Purkayastha, A. B. Das, S. Dhara, *J. Photochem. Photobiol. A: Chem.* **2008**, *199*, 179–187.
[34] S. Nad, PhD Thesis, University of Bombay (Mumbai), **2002**.
[35] E. S. Voropai, M. P. Samtsov, K. N. Kaplevskii, A. A. Maskevich, V. I. Stepuro, O. I. Povarova, I. M. Kuznetsova, K. K. Turoverov, A. L. Fink, V. N. Uverskiid, *J. Appl. Spectrosc.* **2003**, *70*, 868–874.
[36] G. Neunert, P. Polewski, P. Walejko, M. Markiewicz, S. Witkowski, K. Polewski, *Spectrochim. Acta Part A* **2009**, *73*, 301–308.
[37] R. C. Weast, *CRC Handbook of Chemistry and Physics*, CRC Press, Boca Raton, **1970**.
[38] P. E. Liley, T. Makita, Y. Tanaka, *Properties of Inorganic and Organic Fluids* (Ed.: C. Y. Ho), Hemisphere, New York, **1988**.
[39] G. B. Dutt, V. J. P. Srivatsavoy, A. V. Sapre, *J. Chem. Phys.* **1999**, *111*, 9705–9710.
[40] M. J. van der Meer, H. Zhang, M. Glasbeek, *J. Chem. Phys.* **2000**, *112*, 2878–2887.
[41] P. Changenet, H. Zhang, M. J. van der Meer, M. Glasbeek, P. Plaza, M. M. Martin, *J. Phys. Chem. A* **1998**, *102*, 6716–6721.
[42] R. A. Velapoldi, K. D. Mielenz, *Standard Reference Materials: A Fluorescence Standard Reference Material: Quinine Sulfate Dehydrate*, National Bureau of Standards, Gaithersburg, **1980**, pp. 260–264.
[43] J. R. Lackowicz, *Principles of Fluorescence Spectroscopy*, 3rd ed., Springer, New York, **2006**.
[44] S. Nad, M. Kumbhakar, H. Pal, *J. Phys. Chem. A* **2003**, *107*, 4808–4816.
[45] P. K. Singh, S. Nath, A. C. Bhasikuttan, M. Kumbhakar, J. Mohanty, S. K. Sarkar, T. Mukherjee, H. Pal, *J. Chem. Phys.* **2008**, *129*, 114504-1-11.
[46] A. D. Becke, *J. Chem. Phys.* **1993**, *98*, 5648–5652.
[47] C. Lee, W. Yang, R. G. Parr, *Phys. Rev. B* **1988**, *37*, 785–789.
[48] Gaussian 03, Revision C.02, M. J. Frisch, G. W. Trucks, H. B. Schlegel, G. E. Scuseria, M. A. Robb, J. R. Cheeseman, J. A. Montgomery, Jr., T. Vreven, K. N. Kudin, J. C. Burant, J. M. Millam, S. S. Iyengar, J. Tomasi, V. Barone, B. Mennucci, M. Cossi, G. Scalmani, N. Rega, G. A. Petersson, H. Nakatsuji, M. Hada, M. Ehara, K. Toyota, R. Fukuda, J. Hasegawa, M. Ishida, T. Nakajima, Y. Honda, O. Kitao, H. Nakai, M. Klene, X. Li, J. E. Knox, H. P. Hratchian, J. B. Cross, V. Bakken, C. Adamo, J. Jaramillo, R. Gomperts, R. E. Stratmann, O. Yazyev, A. J. Austin, R. Cammi, C. Pomelli, J. W. Ochterski, P. Y. Ayala, K. Morokuma, G. A. Voth, P. Salvador, J. J. Dannenberg, V. G. Zakrzewski, S. Dapprich, A. D. Daniels, M. C. Strain, O. Farkas, D. K. Malick, A. D. Rabuck, K. Raghavachari, J. B. Foresman, J. V. Ortiz, Q. Cui, A. G. Baboul, S. Clifford, J. Cioslowski, B. B. Stefanov, G. Liu, A. Liashenko, P. Piskorz, I. Komaromi, R. L. Martin, D. J. Fox, T. Keith, M. A. Al-Laham, C. Y. Peng, A. Nanayakkara, M. Challacombe, P. M. W. Gill, B. Johnson, W. Chen, M. W. Wong, C. Gonzalez, J. A. Pople, Gaussian, Inc., Wallingford CT, **2004**.
[49] V. Barone, M. Cossi, *J. Phys. Chem. A* **1998**, *102*, 1995–2001.

Received: October 27, 2009
Revised: March 2, 2010
Published online: June 25, 2010

  